Projected Changes in Heavy Precipitation over North America in CMIP5 Climate Model Simulations

RUTGERS
THE STATE UNIVERSITY OF NEW JERSEY

Anthony M. DeAngelis[1], Anthony J. Broccoli[1], and Steven G. Decker[1]
[1]Department of Environmental Sciences, Rutgers University, New Brunswick, NJ
contact: deangelis@envsci.rutgers.edu

Center for Environmental Prediction, Rutgers University

OVERVIEW

Earlier studies using coupled atmosphere-ocean climate models show that heavy precipitation increases over much of North America in a future warmer climate (e.g., Sun et al. 2007, Tebaldi et al. 2006). Allen and Ingram (2002) proposed that increases in heavy precipitation result primarily from increases in atmospheric water vapor in the absence of substantial circulation changes. More recently, O'Gorman and Schneider (2009) developed a scaling in which changes in vertical motion and atmospheric stability are also important in determining the rate of increase of heavy precipitation in response to warming, and Wehner (2012) speculated that changes in atmospheric circulation patterns associated with extreme events are important as well.

Encouraged by the success of CMIP3 models in simulating the circulation features associated with heavy precipitation (DeAngelis et al. 2012), we study precipitation extremes in historical and future climate simulations from CMIP5. Our main goal is to better understand the physical mechanisms that lead to the simulated changes in regional extreme precipitation. We compare our results to a baseline increase of 7%/K, which approximates the rate of increase of low-level atmospheric water vapor if relative humidity is assumed to remain constant, to identify regions in which the rate of increase of heavy precipitation is inconsistent with this simple scaling.

DATA AND METHODOLOGY

- **Models:** Output (daily resolution) from 24 CMIP5 models (one ensemble member from each).
- **Historical:** Simulation of the recent past including observed changes in atmospheric composition, solar forcing, and land use:
  January 1, 1979 – December 31, 1999.
- **RCP85:** Future simulation in which radiative forcing reaches approximately 8.5 W/m^2 by 2100:
  January 1, 2079 – December 31, 2099.
- **Resolution:** A common grid of 2.5°x2.5° lon-lat is used for analysis, where linear interpolation or area averaging was used in the regridding process.

ACKNOWLEDGEMENTS

- We acknowledge the World Climate Research Programme's Working Group on Coupled Modelling, which is responsible for CMIP, and we thank the climate modeling groups for producing and making available their model output. For CMIP the U.S. Department of Energy's Program for Climate Model Diagnosis and Intercomparison provides coordinating support and led development of software infrastructure in partnership with the Global Organization for Earth System Science Portals.
- This work was supported by a fellowship from the Environmental Protection Agency Science to Achieve Results (EPA STAR) program and a grant from the NOAA Climate Program Office.

HEAVY PRECIPITATION CHANGES

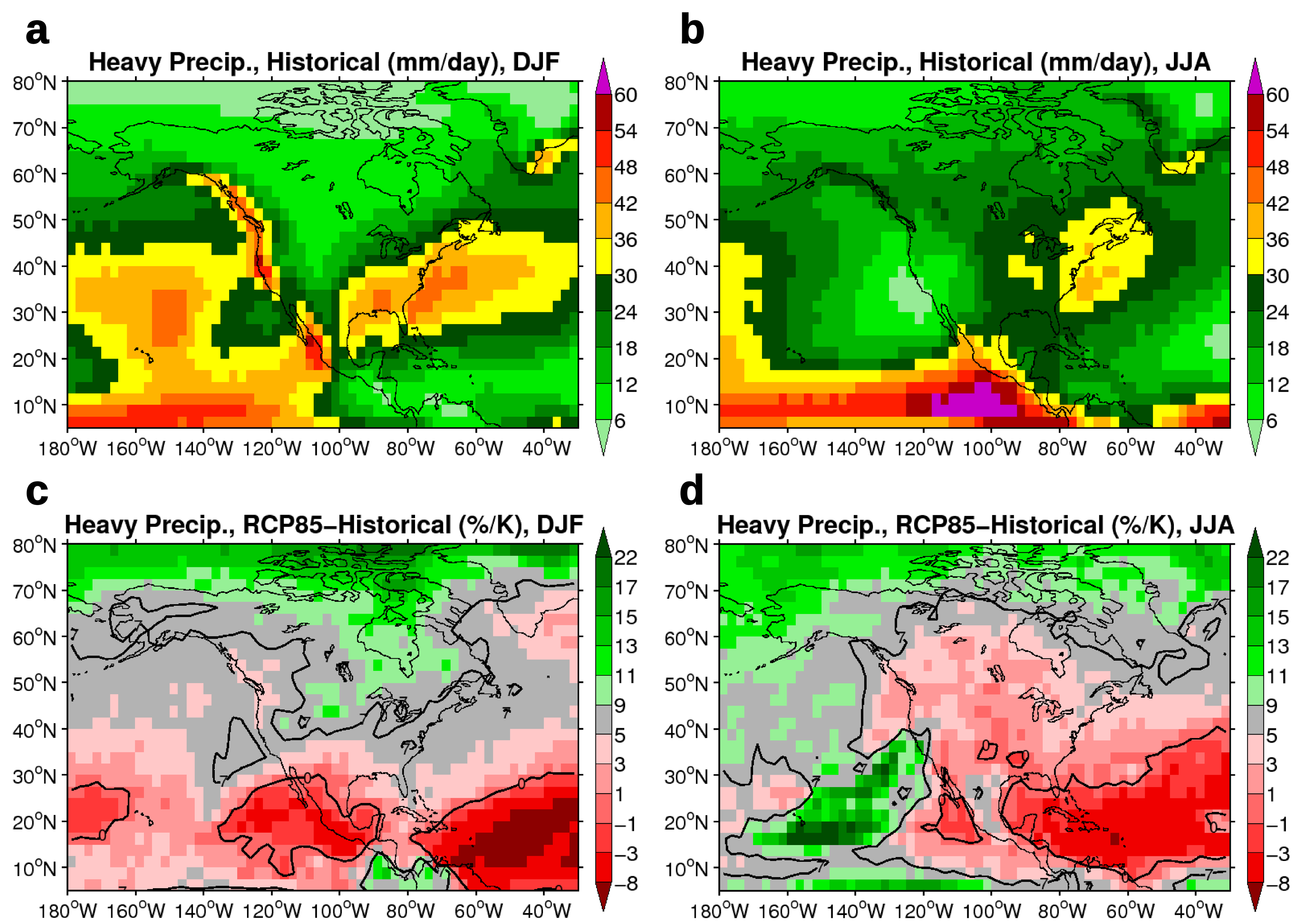

Figure 1. (a,b) Mean precipitation coming from the daily 99th percentile and above (P99M) for the historical simulation for (a) winter and (b) summer. (c,d) The percent change in P99M between the RCP85 and historical simulations, normalized by the area-weighted global average time mean 2m temperature change for (c) winter and (d) summer. In panels (c) and (d), 0 and 7%/K contours are drawn- note that the color bar is centered at +7%/K. Global mean warming is approximately 3-5 K depending on the model and season. The average over all models is shown in all panels.

- The regional pattern of changes in heavy precipitation is consistent with previous studies that used CMIP3 models.
- Changes in heavy precipitation in middle to high latitudes are close to what is expected from increases in atmospheric water vapor, suggesting atmospheric circulation changes are small.

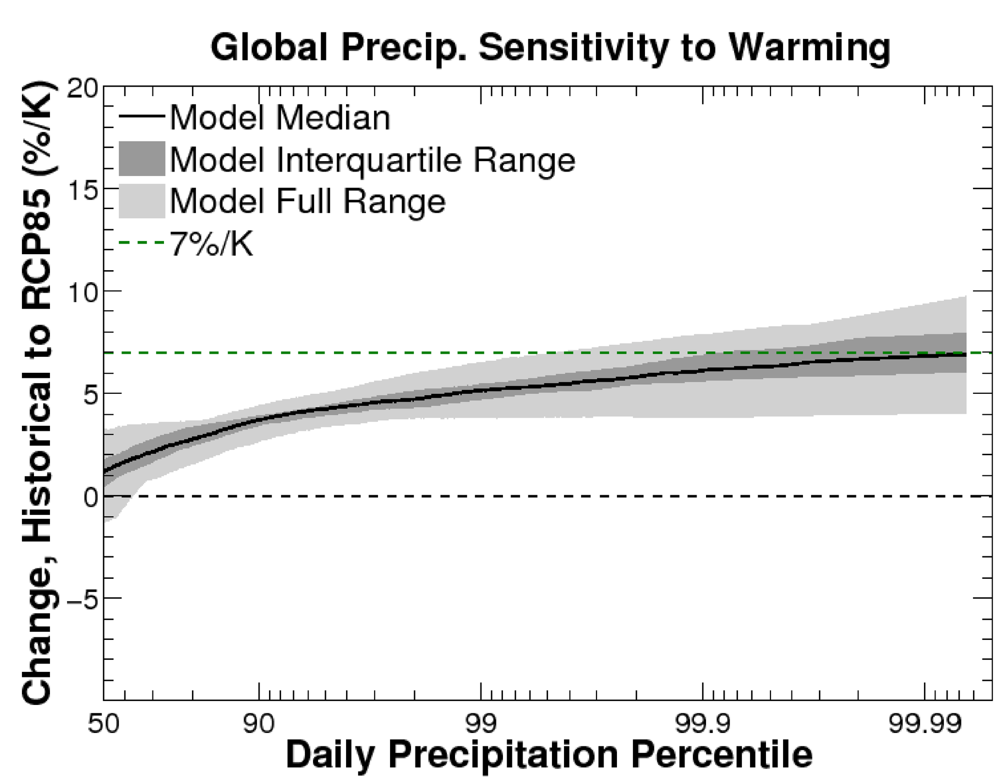

Figure 2. At each grid cell and for each model, the daily precipitation for all days was sorted min to max. The percent difference in sorted precipitation between the RCP85 and historical simulations was computed and divided by the area-weighted global average time mean 2m temperature change to represent a precipitation sensitivity to warming. The median value of all global grid cells was then computed for each model at each percentile. The median model and inter-model variability are depicted on the graph, with a logarithmic abscissa axis.

- The global median sensitivity of daily precipitation to warming approaches 7%/K for the most extreme events, suggesting that increases in low-level moisture act as a global constraint.

PHYSICAL MECHANISMS

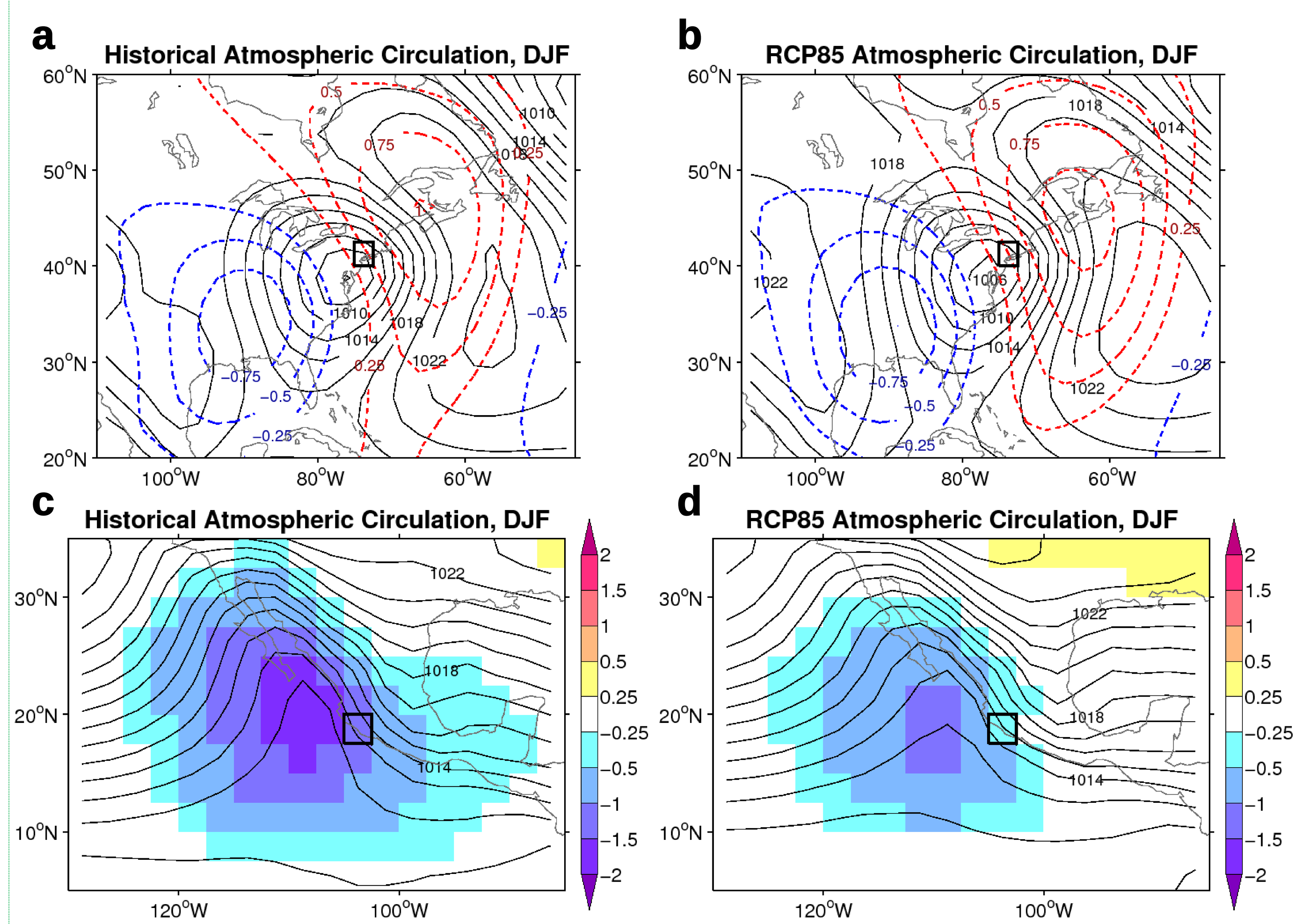

Figure 3. (a,b) The average sea level pressure (hPa, black contours) and 500 mb geopotential height standardized anomaly (dimensionless, dashed contours) for the wettest 21 winter days at the grid cell indicated for the (a) historical and (b) RCP85 simulations. (c,d) As in (a,b) but showing the standardized anomaly of sea level pressure as color fills. The standardized anomalies were computed using a seasonally varying climatology and standard deviation. The RCP85 mean and historical standard deviation were used for the RCP85 plots. All panels show the multi-model average (17 of total 24 models used).

- At middle to high latitude grid cells, where extreme precipitation increases by near 7%/K in the future, atmospheric circulations associated with extreme events do not change substantially.
- Weakening of sea level pressure anomalies during extreme events can be detected in some low latitude grid cells that show decreases in extreme precipitation in the future.

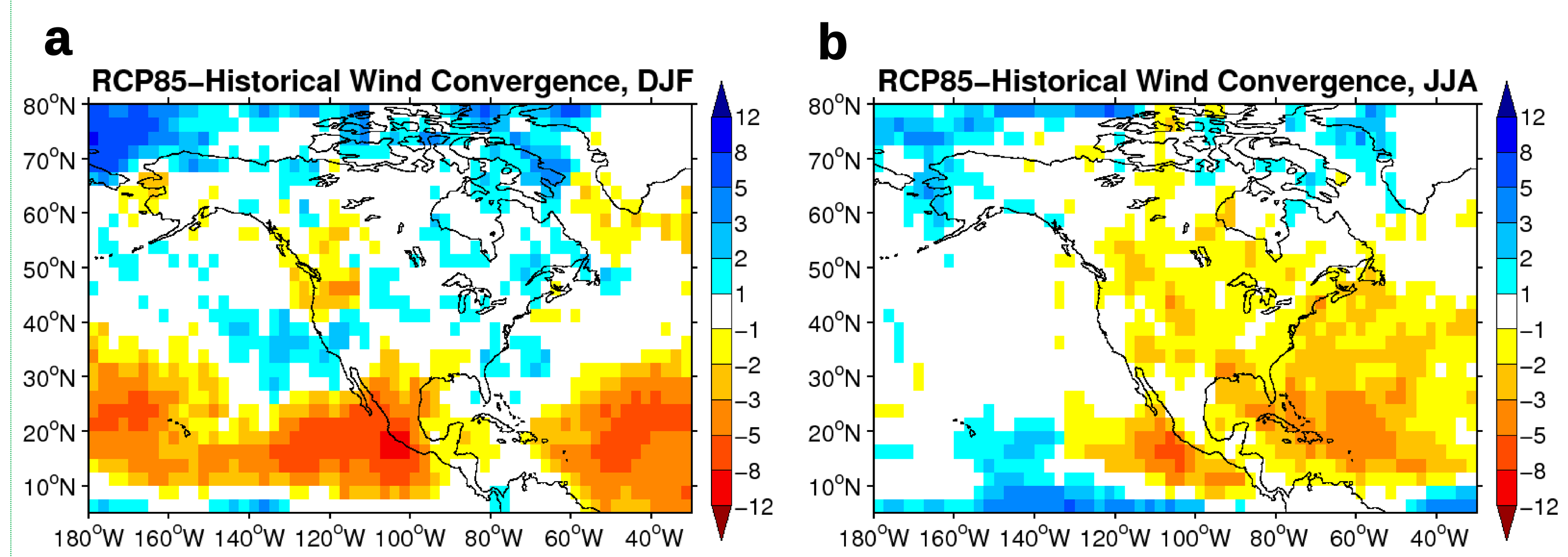

Figure 4. The difference between the RCP85 and historical simulation in the convergence of the vertically integrated wind (surface–600-mb, 10^{-3} $kg/m^2/s$) averaged over the 21 most extreme (a) winter and (b) summer precipitation events at each grid cell on the domain. The multi-model average is shown (17 of total 24 models used).

- Changes in low-level wind convergence during extreme events appear to be correlated with deviations in extreme precipitation changes from 7%/K, particularly in low latitudes. This relationship will be a topic of further investigation.

CMIP5 Overview: WCRP Coupled Model Intercomparison Project – Phase 5: Special Issue of the CLIVAR Exchanges Newsletter, No. 56, Vol. 15, No. 2
CMIP5 Experimental Design: Taylor, K.E., R.J. Stouffer, and G.A. Meehl, 2012: An overview of CMIP5 and the experiment design. *Bull. Amer. Meteor. Soc.*, **93**, 485-498, doi:10.1175/BAMS-D-11-00094.1.
Allen, M. R., and W. J. Ingram, 2002: Constraints on future changes in climate and the hydrologic cycle. *Nature*, **419**, 224-232.
DeAngelis, A. M., A. J. Broccoli, and S. G. Decker, 2012: A comparison of CMIP3 simulations of precipitation over North America with observations: Daily statistics and circulation features accompanying extreme events. *J. Climate*, doi: 10.1175/JCLI-D-12-00374.1, in press.
O'Gorman, P. A., and T. Schneider, 2009: The physical basis for increases in precipitation extremes in simulations of 21st-century climate change. *Proc. Natl. Acad. Sci.* , **106**, 14773-14777.
Sun, Y., S. Solomon, A. Dai, and R. W. Portmann, 2007: How often will it rain? *J. Climate*, **20**, 4801-4818, doi:10.1175/JCLI4263.1.
Tebaldi, C., K. Hayhoe, J. M. Arblaster, and G. A. Meehl, 2006: Going to the extremes: An intercomparison of model-simulated historical and future changes in extreme events. *Climatic Change*, **79**, 185-211, doi: 10.1007/s10584-006-9051-4.
Wehner, M. F., 2012: Very extreme seasonal precipitation in the NARCCAP ensemble: model performance and projections. *Climate Dyn.*, doi: 10.1007/s00382-012-1393-1.

Modeling Group	Model Name	Lon. (°)	Lat. (°)
Commonwealth Scientific and Industrial Research Organization (CSIRO) and Bureau of Meteorology (BOM) (Australia)	ACCESS1.0	1.88	1.24
Beijing Climate Center, China Meteorological Administration (China)	BCC-CSM1.1*	2.81⁺	2.81⁺
College of Global Change and Earth System Science, Beijing Normal University (China)	BNU-ESM	2.81⁺	2.81⁺
Canadian Centre for Climate Modelling and Analysis (Canada)	CanESM2*	2.81⁺	2.81⁺
National Center for Atmospheric Research (USA)	CCSM4 (r6)	1.25	0.94
Centro Euro-Mediterraneo per I Cambiamenti Climatici (Italy)	CMCC-CM	0.75	0.75
Centre National de Recherches Meteorologiques / Centre Europeen de Recherche et Formation Avancees en Calcul Scientifique (France)	CNRM-CM5*	1.41	1.41
Commonwealth Scientific and Industrial Research Organization in collaboration with Queensland Climate Change Centre of Excellence (Australia)	CSIRO-Mk3.6.0*	1.88	1.88
LASG, Institute of Atmospheric Physics, Chinese Academy of Sciences (China)	FGOALS-s2*	2.81	1.67
NOAA Geophysical Fluid Dynamics Laboratory (USA)	GFDL-ESM2G*	2.50	2.00
	GFDL-ESM2M*	2.50	2.00
Met Office Hadley Centre (UK)	HadGEM2-CC*	1.88	1.25
	HadGEM2-ES	1.88	1.24
Institute for Numerical Mathematics (Russia)	INM-CM4*	2.00	1.50
Institut Pierre-Simon Laplace (France)	IPSL-CM5A-LR*	3.75⁺	1.88⁺
	IPSL-CM5A-MR*	2.50	1.26
	IPSL-CM5B-LR	3.75⁺	1.88⁺
Atmosphere and Ocean Research Institute (The University of Tokyo), National Institute for Environmental Studies, and Japan Agency for Marine-Earth Science and Technology (Japan)	MIROC5*	1.41	1.41
Japan Agency for Marine-Earth Science and Technology, Atmosphere and Ocean Research Institute (The University of Tokyo), and National Institute for Environmental Studies (Japan)	MIROC-ESM*	2.81⁺	2.81⁺
	MIROC-ESM-CHEM*	2.81⁺	2.81⁺
Max Planck Institute for Meteorology (Germany)	MPI-ESM-LR*	1.88	1.88
	MPI-ESM-MR*	1.88	1.88
Meteorological Research Institute (Japan)	MRI-CGCM3*	1.13	1.13
Norwegian Climate Centre (Norway)	NorESM1-M	2.50	1.88

List of the CMIP5 models used for analysis in this poster. The approximate spatial resolutions (Lon. and Lat. columns) were calculated by dividing 360° or 180° by the number of grid cells in the longitude or latitude dimensions, respectively. The first ensemble member run (except for the NCAR-CCSM4, in which run 6 was used) was used from each model.

*** Indicates the 17 models that were used for the atmospheric circulation analysis (right column on poster) due to output availability. All 24 models were used for the precipitation analysis (middle column on poster).**

⁺ Indicates the model grids that were transformed to the common 2.5°x2.5° lon-lat resolution using linear interpolation due the coarse native grid. All others were transformed using area averaging.